Journal of Applied Polymer Science

Blends of polylactide and poly(3-hydroxybutyrate-*co*-3-hydroxyvalerate) with low content of hydroxyvalerate unit: Morphology, structure, and property

Qingsheng Liu,[1,2,3,4] Cong Wu,[1] Hongxia Zhang,[5] Bingyao Deng[1]

[1]Key Laboratory of Eco-Textiles, Ministry of Education, Jiangnan University, Wuxi 214122, China
[2]The Key Laboratory of Food Colloids and Biotechnology, Ministry of Education, Jiangnan University, Wuxi 214122, China
[3]State Key Laboratory of Molecular Engineering of Polymers, Fudan University, Shanghai 200433, China
[4]Key Laboratory of Yarn Forming and Combination Processing Technology of Zhejiang Province, Jiaxing University, Jiaxing 314001, China
[5]Wuxi Entry-Exit Inspection and Quarantine Bureau, Wuxi 214101, China
Correspondence to: Q. Liu (E-mail: qsliu@jiangnan.edu.cn) and B. Deng (E-mail: bydeng168@163.com)

ABSTRACT: The Polylactide (PLA)/poly(3-hydroxybutyrate-*co*-3-hydroxyvalerate) (PHBV) blends with four different weight ratios were prepared by melt mixing. PLA and PHBV in PLA/PHBV blends were immiscible while the weak interaction between PLA and PHBV existed. The PHBV domains below 2 μm were dispersed in PLA matrix uniformly. The addition of PHBV made the crystallization of PLA easier due to PHBV acting as nucleating agent. PLA spherulites in PLA/PHBV blends presented various banded structures. In addition, the crystallinity of neat PLA was lower than those of PLA/PHBV blends. With the increase of PHBV content in PLA/PHBV blends, the crystallinity of PLA/PHBV blends increased. PHBV could enhance significantly the toughness of PLA. However, with the increase of PHBV content, the yield stress (σ_y), tensile modulus (E), and the yield strain (ε_y) of PLA/PHBV blends decreased gradually. In addition, incorporation of PHBV to PLA caused a transformation from an optical transparent to an opaque system. © 2015 Wiley Periodicals, Inc. J. Appl. Polym. Sci. **2015**, *132*, 42689.

KEYWORDS: biodegradable; blends; mechanical properties

Received 5 March 2015; accepted 2 July 2015
DOI: 10.1002/app.42689

INTRODUCTION

Polylactide (PLA) with good biodegradability and biocompatibility is a type of thermoplastic polyester synthesized from renewable resources.[1–4] PLA among the family of biomass-derived biodegradable polymers has relatively high strength and modulus.[5] PLA can be used widely as many disposable products such as baby diapers and plastic bags as well as some traditional products such as industrial devices, packaging, film, and fiber materials.[1–5] In addition, PLA can be used in medical materials including implant materials, surgical suture, and controlled drug delivery systems because it degrades to nontoxic lactic acid, which is naturally present in the human body.[1–5] However, PLA is brittle, which restricts its large-scale commercial applications.[5]

The toughness of PLA can be improved by different methods including copolymerization and blending, among which blending is a less expensive and more practical strategy to overcome the drawback of PLA.[6] Therefore, various polymers including renewable, biodegradable, and biocompatible poly(3-hydroxybutyrate-*co*-3-hydroxyvalerate) (PHBV) were used to blend with PLA.[7,8] PHBV is synthesized by many bacteria as an intracellular carbon and energy compound, which can be used as environmental friendly materials and biomedical materials such as controlled release, surgical sutures, wound dressings, lubricating powders, and tissue engineering.[9–16] However, PHBV is brittle, which makes it not necessarily well-suited for certain applications.[9–16] The reasons for brittleness of PHBV are as follow. First, PHBV owned high crystallinity. Second, the circular breaks around the center and cracks in the radial direction of PHBV spherulites appear. However, it was surprising that the toughness of PLA could be improved by introducing PHBV with high brittleness. Ma *et al.*[17] introduced PHBV with 40 mol % HV to PLA. The toughness of PLA was improved greatly. Neat PLA presented a typical brittle fracture. However, PLA/PHBV blends were ductile after addition of 10–30 wt % of the PHBV. When the content of PHBV was 20 wt %, elongation at break of PLA/PHBV blend was close to 300%. However, the HV content of commercial available PHBV is below 15 mol %.[11,15] Therefore,

it is meaningful that the commercial available PHBV is selected to study the effect of PHBV on mechanical property of PLA. Zhang *et al.*[18] and Abdelwahab *et al.*[19] studied the effect of 25 and 50 wt % PHB with 0 mol % HV on the mechanical property of PLA. Modi *et al.*[20] and Nanda *et al.*[21] investigated the effect of 50 wt % PHBV with low HV content on the mechanical property of PLA. However, it can be seen from previous Refs. 18–21 that only 25 and 50 wt % PHB or PHBV with low HV content were selected to blend with PLA. The blends with other ratios were not studied so that it was difficult for us to understand completely the effect of PHBV with relatively low HV content on the structure and properties of PLA.

Therefore, in this article, PHBV with low HV content was selected to blend with PLA. The crystallization and melting behaviors, the miscibility and interaction between PLA and PHBV, phase morphology, mechanical property, and optical transparency of PLA/PHBV blends with the ratios of 95/5, 90/10, 80/20, and 70/30 were studied in detail.

EXPERIMENTAL

Material Preparation

Polylactide (PLA) was supplied from Natureworks, USA under the trade name 4032D. Poly(3-hydroxybutyrate-*co*-3-hydroxyvalerate) (PHBV) was produced from Tianan Biological Materials, China and commercialized in powder form under the trade name ENMAT Y 1000. The HV content was about 5.0 mol %.

The PLA and PHBV were dried at 65°C for 48 h in vacuum oven before processing. The blends were prepared by melt mixing in a SJSZ-10A two-screw microcompounder (Wuhan Rayzone Ming Plastics Machinery, Ltd.). Polymers were mixed at screw speed of 20 rpm for 4 min at 180°C. The weight percent of PHBV in the resulting blends ranged from 5 to 30 wt %. In addition, the neat PLA was subjected to the same mixing treatment so that neat PLA had the same thermal history as the blends.

Differential Scanning Calorimetry

The crystallization behaviors and melting behaviors of samples were characterized by differential scanning calorimetry (DSC) that used a DSC Q200 (TA Instruments®). Nitrogen was used at a flow rate of 50 mL/min. The instrument was calibrated with In and Pb. The weight of the samples was in the range of 4–6 mg.

Hot-Stage Polarized Microscope

The samples were placed between crossed polarizers in a Leica optical microscope (DM2700P) with a CCD camera. They were melted at 220°C (200°C for PHBV) for 3 min and then quickly cooled at the rate of 100°C/min to the isothermal crystallization temperature (120°C for pure PLA and PLA composition in PLA/PHBV blends, 50°C for pure PHBV) in a hot-stage LINKAM TMS420 for morphological observation of the samples.

Fourier Transform Infrared Attenuated Total Reflection Spectroscopy

Spectra of fourier transform infrared attenuated total reflection (FTIR–ATR) were recorded on a Nicolet FTIR spectroscope (Nexus 670). Each spectrum was recorded with a total of 16 scans; each had a resolution of 4 cm^{-1} at room temperature. Software of OMNIC Nicolet was used for spectra analysis.

Scanning Electron Microscope

Scanning electron microscope (SEM) measurements of cross-section of cryogenically fractured samples in liquid nitrogen were carried out with a Model S-4800 field emission scanning electron microscope (Hitachi, Japan). The samples were broken into pieces in liquid nitrogen, and then were sputtered with gold. SEM measurements of the fractured samples obtained after tensile testing were carried out with a Model SU1510 scanning electron microscope (Hitachi, Japan). The samples were sputtered with gold.

Mechanical Property

Tensile properties were determined on Instron 3385H tensile strength test machine using rectangle specimens at room temperature. The rectangle specimens with a dimension of 100 × 20 × 1 mm^3 were prepared by hot pressing at 180°C, 8 MPa for 3 min on a CARVER hot press machine (Carver, Wabash, IN). The cross-head speed and gauge length of the apparatus were 5 mm/min and 50 mm, respectively.

Optical Transparency

The samples with the thickness of 1mm were by hot pressing at 180°C, 8 MPa for 3 min on a CARVER hot press machine (Carver, Wabash, IN). The images were obtained using a Nikon (COOLPIX 990) digital camera.

RESULTS AND DISCUSSION

Nonisothermal Crystallization and Melting Behaviors

To explore the effect of PHBV on the crystallinity of PLA/PHBV blends, the PLA/PHBV blends, and the neat PLA were heated from 0 to 190°C at 10°C/min using DSC. The corresponding first heating DSC curves were shown in Figure 1(a). The $\Delta H_m - \Delta H_{cc}$ for a sample could be calculated from corresponding DSC curve also was listed in Table I. The larger the $\Delta H_m - \Delta H_{cc}$ is, the higher the crystallinity is. It could be seen from Table I that the $\Delta H_m - \Delta H_{cc}$ of neat PLA was nearly 0, which showed that neat PLA was amorphous completely. The $\Delta H_m - \Delta H_{cc}$ of PLA/PHBV blends was larger than that of neat PLA. With the increase of PHBV content, $\Delta H_m - \Delta H_{cc}$ of PLA/PHBV blends increased gradually. In other words, introducing PHBV to PLA enhanced the crytallinity of PLA/PHBV blends. It is well known that the brittleness of PLA has been mainly attributed to the rapid physical aging of the polymer under ambient temperature (about 25°C) below the T_g.[8] Aging below T_g is exclusively related to the amorphous phase of the polymer; accordingly, increasing the crystallinity of the polymer will reduce the aging effect.[2,8] Furthermore, the crystallites formed also act like physical crosslinks to retard the polymer chain mobility.[2,8] Therefore, it was probable that the improvement of toughness of PLA by introducing PHBV was partly due to the increase of crystallinity of PLA/PHBV blends in comparison with neat PLA.[2,8]

Figure 1(b) showed the second heating DSC curves of PLA/PHBV blends and corresponding neat polymers at 10°C/min prepared by quenching the melts to −90°C at 100°C/min. In the heating DSC curves of neat PLA, the T_g, the cold-crystallization temperature (T_{cc}) and the melting temperature (T_m) were observed at 57.2, 109.4, and 168.6/161.0°C,

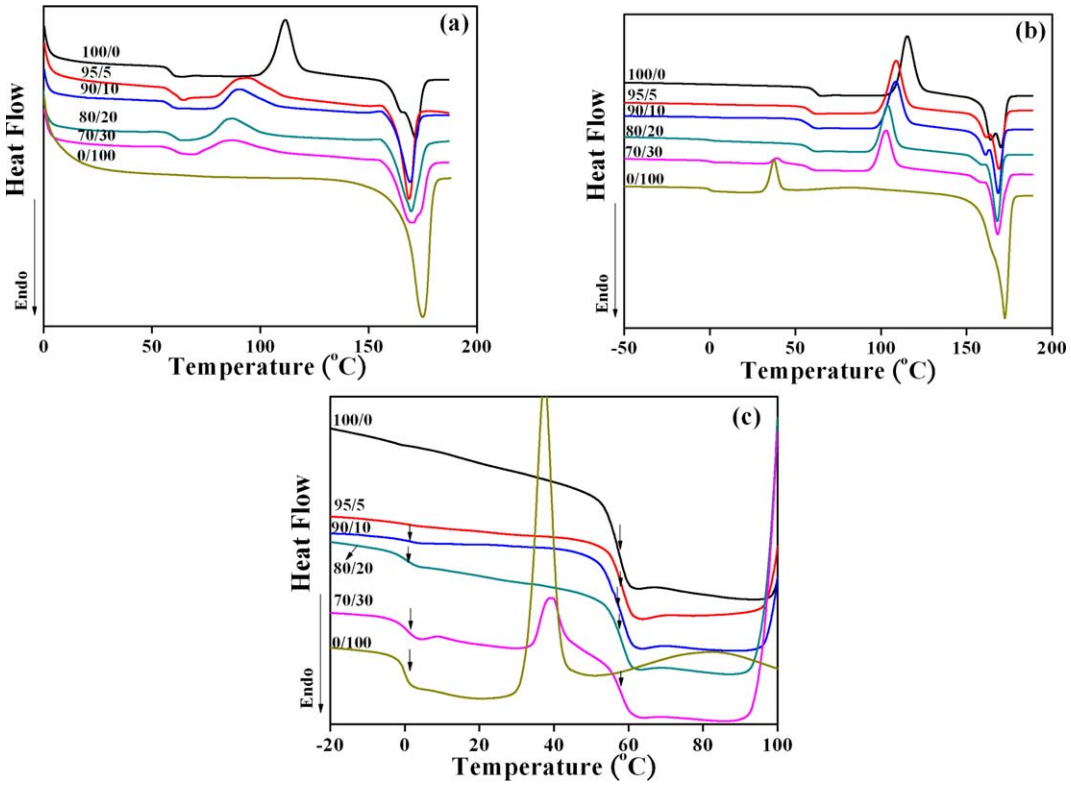

Figure 1. The DSC curves of PLA/PHBV blends and corresponding neat polymers. (a) The first heating process at 10°C/min, (b) the second heating process at 10°C/min from −50 to 200°C, (c) the second heating process at 10°C/min from −20 to 100°C. [Color figure can be viewed in the online issue, which is available at wileyonlinelibrary.com.]

respectively. In the heating DSC curves of neat PHBV, the T_g, T_{cc}, and T_m were observed at 0.0, 37.5, and 172.3°C, respectively. On the basis of the second heating DSC curves of neat polymers, it was easy to distinguish the characteristic temperatures of blends. The T_gs near 0 and 60°C was attributed to mobility of molecule segments of PHBV and PLA components, respectively. To observe clearly the glass transition of PLA and PHBV component of PLA/PHBV blends, the enlargement of the DSC curves from −20 to 100°C was shown in Figure 1(c). The exothermic peaks near 40 and 110°C were attributed to cold-crystallization of PHBV and PLA components, respectively. It was known from Figure 1(a) that the $T_{m(PLA)}$ of neat PLA was close to $T_{m(PHBV)}$ of neat PHBV. Therefore, the melting peaks near 170°C in the DSC heating curves of PLA/PHBV blends were attributed to the overlapping of melting peaks of PLA and PHBV components. The data of $T_{g(PLA)}$, $T_{g(PHBV)}$, $T_{cc(PLA)}$, $T_{cc(PHBV)}$, $T_{m(PLA)}$, and $T_{m(PHBV)}$ were listed in Table I. The miscibility of blends was often analyzed by characterizing the T_g using DSC. It could be seen from Figure 1(c) that for PLA/PHBV blend with 5 wt % PHBV, only the $T_{g(PLA)}$ could be observed while the $T_{g(PHBV)}$ could not be observed because of low content of PHBV. For other PLA/PHBV blends, both $T_{g(PLA)}$ and $T_{g(PHBV)}$ appeared. Figure 1(b) and Table I showed that T_gs of PLA and PHBV components of PLA/PHBV blends were almost equal to those of corresponding neat polymers. Therefore, it was concluded that PLA and PHBV in PLA/PHBV blends were immiscible. The result was accorded with the ones obtained by Nanda *et al.*[21]

Figure 1(b) and Table I showed that $T_{cc(PLA)s}$ of blends were lower than that of neat PLA, which illustrated that the crystallization of PLA became easier by introducing PHBV as a nucleating agent. In addition, with the increase of PHBV content, the

Table I. The Parameters of Cold-Crystallization and Melting Behaviors of PLA/PHBV Blends and Corresponding Neat Polymers

	$T_{g(PLA)}$ (°C)	$T_{g(PHBV)}$ (°C)	$T_{cc(PLA)}$ (°C)	$T_{cc(PHBV)}$ (°C)	T_m (°C)	$\Delta H_m - \Delta H_{cc}$ (J/g)
100/0	57.2	-	109.4	-	168.6/161.0	0.0
95/5	58.4	-	108.8	-	168.8/161.5	9.3
90/10	58.5	1.5	108.6	-	168.4/161.2	10.7
80/20	58.1	0.6	103.9	-	168.0/157.7	17.8
70/30	58.1	0.3	102.8	39.6	168.2/157.7	23.6
0/100	-	0.0	-	37.5	172.3	-

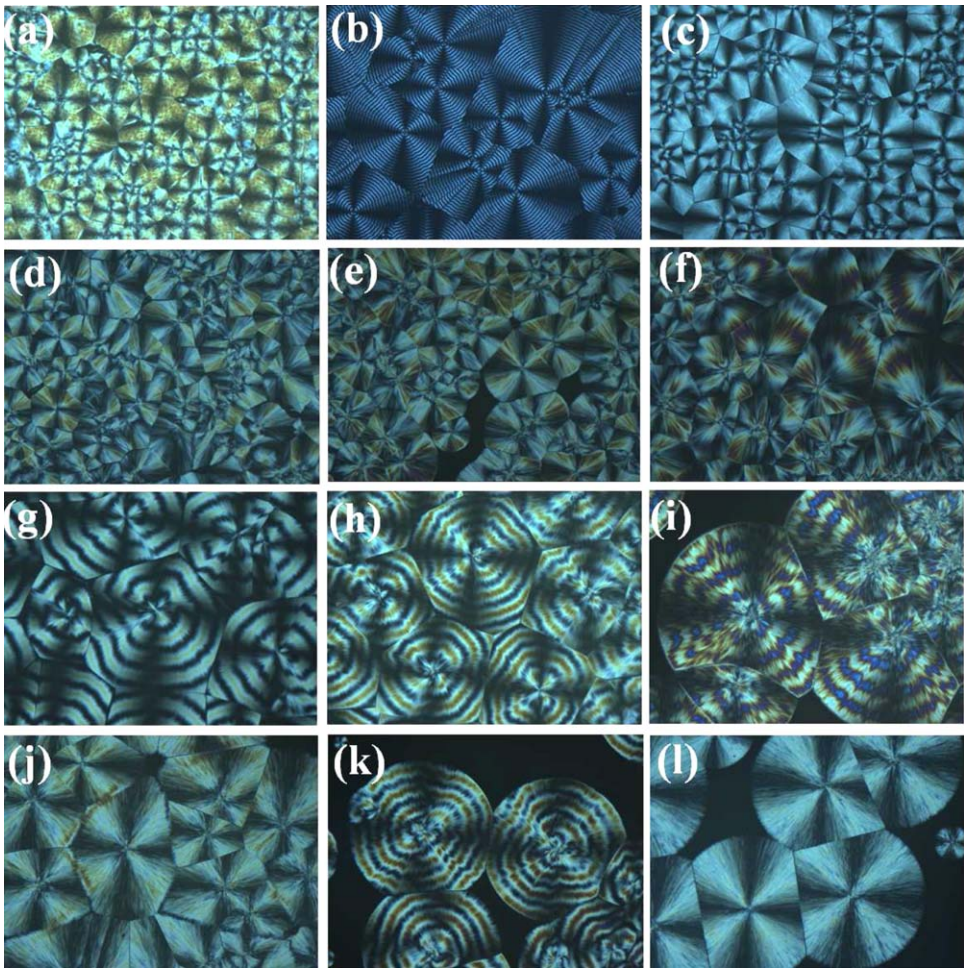

Figure 2. POM photographs of PLA spherulites in PLA/PHBV blends and corresponding neat polymers observed under isothermal melt-crystallization at 120°C for PLA or 50°C for PHBV. (a) Neat PLA; (b) neat PHBV; (c, d) PLA/PHBV = 95/5; (e, f) PLA/PHBV = 90/10; (g, h, i, j) PLA/PHBV = 80/20; and (k, l) PLA/PHBV = 70/30. [Color figure can be viewed in the online issue, which is available at wileyonlinelibrary.com.]

$T_{cc(PLA)s}$ of blends decreased. Figure 1(b) and Table I illustrated that for a sample, double melting peaks or a main melting peak with a shoulder appeared, probably because of the melting of unstable crystals produced during cold crystallization, their recrystallization to form perfect crystals, and the melting of perfect crystals. The melting point from the higher temperature endotherm was taken as the true melting temperature.[16] It could be seen from Figure 1(b) and Table I that the T_ms of PLA/PHBV blends were close to that of neat PLA and lower than that of neat PHBV, which showed that introducing PHBV to PLA almost did not alter the T_m of PLA component. In addition,with the increase of PHBV content, the intensity of the melting peak or the shoulder at the lower temperature decreased, which showed that the content of the unstable crystals produced during cold crystallization decreased while that of perfect crystals increased by introducing PHBV as a nucleating agent.

Spherulite Morphology

Figure 2 illustrated POM photographs of PLA spherulites in PLA/PHBV blends and corresponding neat polymers observed under isothermal melt-crystallization at 120°C for PLA or 50°C for PHBV. Figure 2(a) showed spherulite morphology of neat PLA, which was classic spherulite with the Maltese cross. It can be seen from Figure 2(b) that the spherulites of neat PHBV owned banded structure. Two kinds of spherulite morphology with the Maltese cross were observed in PLA/PHBV blend with 5 wt % PHBV [Figure 2(c,d)], which were different from those of neat PLA. It is surprising that different banded spherulites appeared in PLA/PHBV blends with 10 wt % [Figure 2(f)], 20 wt % [Figure 2(g–i)], and 30 wt % [Figure 2(k)] PHBV expect that common spherulites [Figure 2(e,j,l)] could be observed. The reasons that the spherulites with different morphologies appeared would be further explored in our next work.

FTIR Analysis

Figure 3 showed the FTIR–ATR spectra of PLA/PHBV blends and corresponding neat polymers from 4000 to 800 cm^{-1}. In Figure 3(a), for neat PLA, the C═O stretching band occurred at 1750 cm^{-1}.[22,23] The bands at 2996 and 2944 cm^{-1} were assigned to CH_3 asymmetric and symmetric vibration, respectively.[22,23] The band at 2879 cm^{-1} was assigned to CH vibration. The peaks at 1455 and 1384 cm^{-1} were assigned to CH_3 asymmetric deformation and CH_3 symmetric deformation,

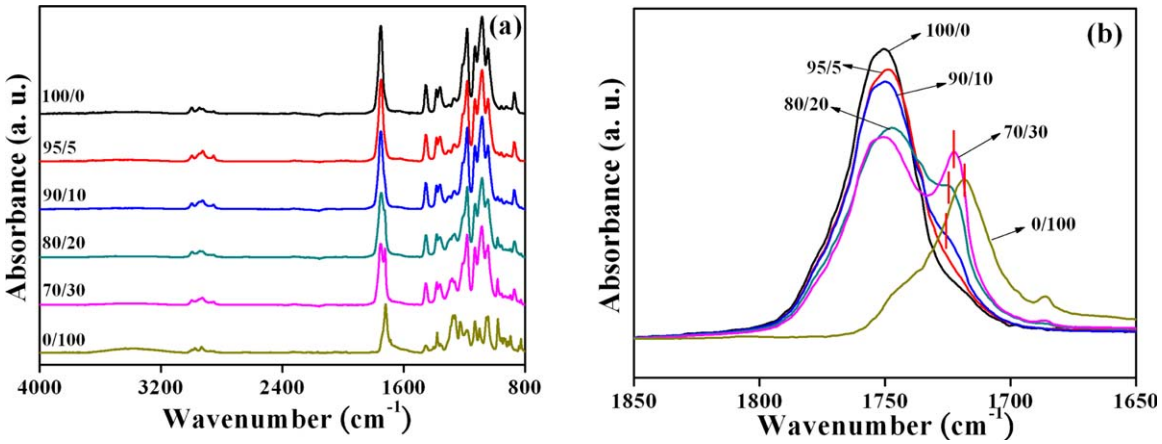

Figure 3. FTIR–ATR spectra of PLA/PHBV blends and corresponding neat polymers. (a) 4000–800 cm^{-1} and (b) 1850–1650 cm^{-1}. [Color figure can be viewed in the online issue, which is available at wileyonlinelibrary.com.]

respectively.[22,23] The peak at 1359 cm^{-1} was assigned to CH deformation and crystalline CH_3 symmetric deformation. The peaks at 1265 cm^{-1} were assigned to C—O—C stretching band and amorphous CH deformation. The peaks at 1181, 1129, 1083, and 1043 cm^{-1} were attributed to C—O—C stretching, CH_3 rocking, C—O—C stretching, and C—CH_3 stretching, respectively.[22,23] For PHBV, the bands in the 3015–2960, 2945–2925, and 2885–2865 cm^{-1} regions were assigned to CH_3 asymmetric stretching modes, CH_2 antisymmetric stretching modes, and CH_3 symmetric stretching modes, respectively.[15] The peak near 1718 cm^{-1} corresponded to C=O stretching modes.[15,22] The bands around 1500–800 cm^{-1} corresponding to the CH_3 and CH bending vibrations and the C—O—C and C—C stretching vibrations were heavily overlapped, and band assignments were not straightforward.[15] It could be seen from Figure 3(a) that main characteristic peaks of PLA and PHBV existed in the FTIR spectra of PLA/PHBV blends. However, some changes appeared in the FTIR spectra of PLA/PHBV blends. To observe clearly the change of C=O peaks, the bands at 1850–1650 cm^{-1} were presented in Figure 3(b). Figure 3(b) showed that a characteristic peak at 1747–1751 cm^{-1} in a PLA/PHBV blend existed, which was obviously attributed to C=O in PLA component. However, with the increase of content of PHBV, a shoulder or an obvious peak existed in PLA/PHBV blends with 10–30 wt % PHBV, which appeared at 1726 (90/10), 1725 (80/20), and 1723 (70/30), respectively, which was obviously due to introducing PHBV. However, the characteristic peak of C=O in neat PHBV appeared at 1718 cm^{-1}. This showed that the characteristic peaks of C=O of PHBV component in PLA/PHBV blends shifted to high wave number, which illustrated that interaction between PLA and PHBV existed. Zembouai *et al.*[24] thought that the interaction was due to change of local molecular environment during crystallization. Zhang *et al.*[25] and Modi *et al.*[20] thought that these interactions between PHBV and PLA were due to weak bonding between α-methylene groups of PHBV to carboxylic group of PLA. Zhang *et al.*[18] studied the blends of PLA and PHB. They thought that the interaction between PLA and PHB was due to the transesterification reaction between PHB and PLA during processing.

Phase Morphology

Figure 4 represented the SEM photos of the PLA/PHBV blends with various PHBV contents. All of the blends showed a clear, phase-separated morphology with PHBV dispersed in PLA matrix uniformly, which illustrated that the miscibility between PLA and PHBV was poor. With the increase of PHBV content, the number of dispersed phase increased gradually. However, for all the blends with 5–30 wt % PHBV, the size of PHBV domain was less than 2 μm. In addition, the parts located in white square frame in Figure 4 were enlarged, which were showed in the upper right corners of SEM photos, respectively so that the morphologies of blends could be observed clearly. It can be seen that the interface between PLA matrix and PHBV disperse phase was obscure, which indicated that the interaction between PLA and PHBV existed. The result was accorded with that of FTIR–ATR analysis.

Mechanical Property

Figure 5 presented stress-strain curves of PLA/PHBV blends and neat PLA. The corresponding parameters of mechanical property were listed in Table II. Figure 5 illustrated that for neat PLA, when the stress reached the maximum value during drawing, the sample broke suddenly, which presented a typical brittle fracture. The break strength (σ_b) and elongation at break (ε_b) were 107 MPa and 4.1%, respectively. For the PLA/PHBV = 95/5 blend, when the stress reached the maximum value (101 MPa) during drawing, the sample did not break and the corresponding strain was 4.2%. When the strain reached 4.5%, the sample broke and the corresponding stress was 84 MPa, which was much smaller than the maximum value. When the content of PHBV was above 10 wt %, for a PLA/PHBV blend, the obvious yield point existed and the ε_b increased obviously (more than 12%) in comparison with neat PLA and PLA/PHBV = 95/5 blend. However, it was difficult to determine the break point of PLA/PHBV blends with more than 10 wt % PHBV so that the specific values of σ_b and ε_b were not listed in Table II. For all the blends, strain softening existed while strain hardening did not happen during drawing. In addition, the yield stress (σ_y) and tensile modulus (E) of PLA/PHBV blends were smaller than the σ_b of neat PLA. For PLA/PHBV blends,

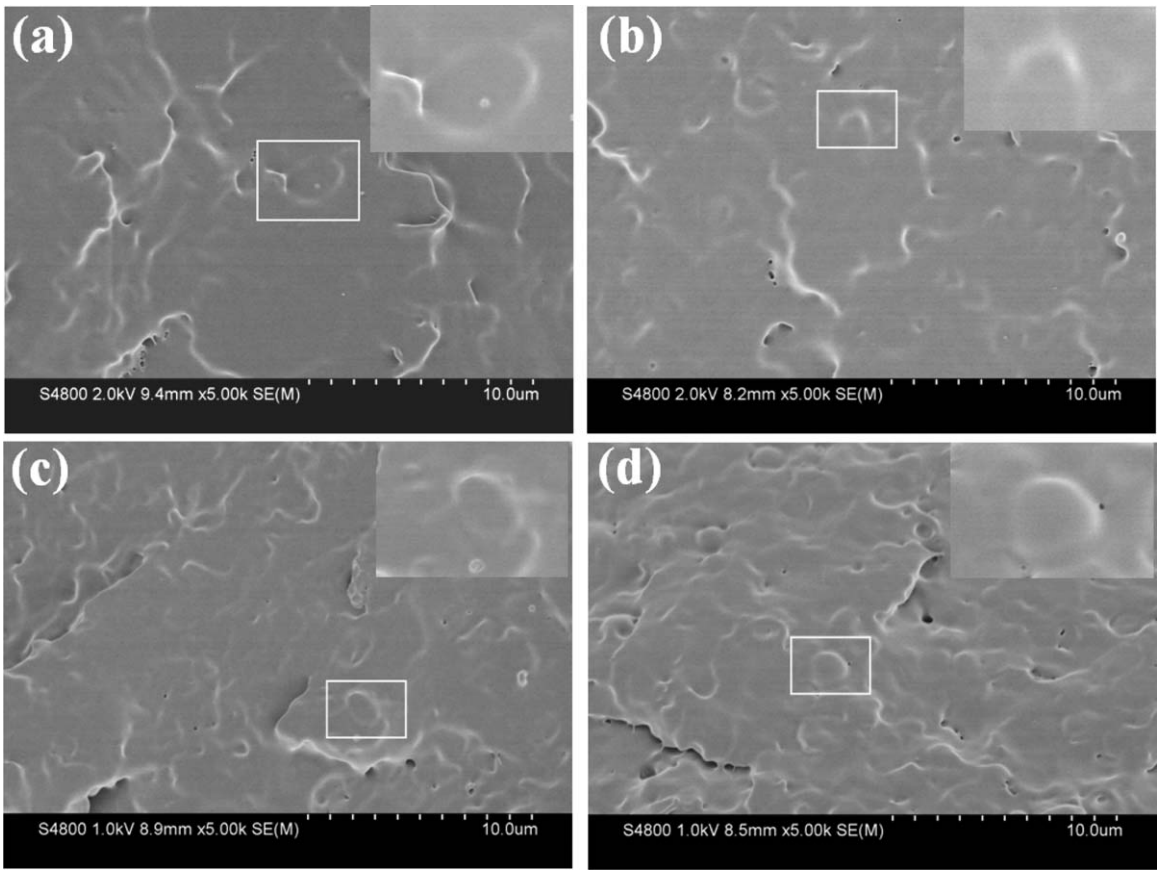

Figure 4. SEM photographs of cryogenically fractured cross-section of PLA/PHBV blends. (a) PLA/PHBV = 95/5, (b) PLA/PHBV = 90/10, (c) PLA/PHBV = 80/20, and (d) PLA/PHBV = 70/30.

with the increase of PHBV content, the σ_y, E, and the yield strain (ε_y) decreased gradually.

Figure 6 illustrated the SEM photographs of tensile-fractured cross-section of PLA/PHBV blends neat PLA. Figure 6(a,a′) indicated that the tensile-fractured cross-section of neat PLA was flat, indicating the neat PLA underwent brittle fracture. The tensile-fractured cross-section of PLA/PHBV blends with 5 wt % PHBV [Figure 6(b,b′)] was a bit rougher than that of neat PLA. When the content of PHBV was more than 10%, the tensile-fractured cross-section of PLA/PHBV blends presented a large degree of matrix deformation [Figure 6(c–e′)], indicating that a brittle-to-ductile transition occurred in the presence of PHBV. The results were similar to those of PLA/novel sliding graft copolymer/methylene diphenyl diisocyanate blends studied by Li *et al.*[26] In addition, some void appeared in tensile-fractured cross-section of PLA/PHBV blends with more than 10 wt % PHBV. It is possible that void formation was one of reasons of enhancement of PLA toughness. The other probable reason for improvement of PLA by introducing PHBV was as followed. The Young's modulus and Poisson's ratio of the rigid PHBV are different from those of the rigid PLA, which resulted

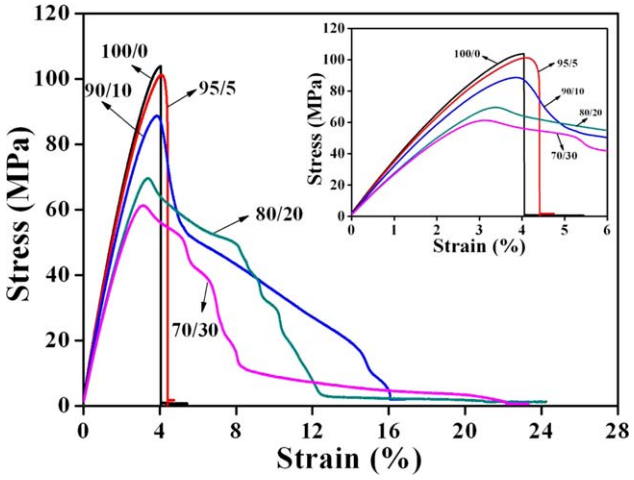

Figure 5. Stress–strain curves of PLA/PHBV blends and neat PLA. [Color figure can be viewed in the online issue, which is available at wileyonlinelibrary.com.]

Table II. The Parameters of Mechanical Properties of PLA/PHBV Blends and Neat PLA

	σ_y (MPa)	ε_y (%)	σ_b (MPa)	ε_b (%)	E (GPa)
100/0	-	-	107 ± 5	4.1 ± 0.6	3.6 ± 0.1
95/5	101 ± 3	4.2 ± 0.1	84 ± 4	4.5±0.1	3.2 ± 0.1
90/10	86 ± 3	3.8 ± 0.1	-	-	2.8 ± 0.1
80/20	71 ± 4	3.1 ± 0.5	-	-	2.6 ± 0.1
70/30	63 ± 3	3.1 ± 0.2	-	-	2.6 ± 0.1

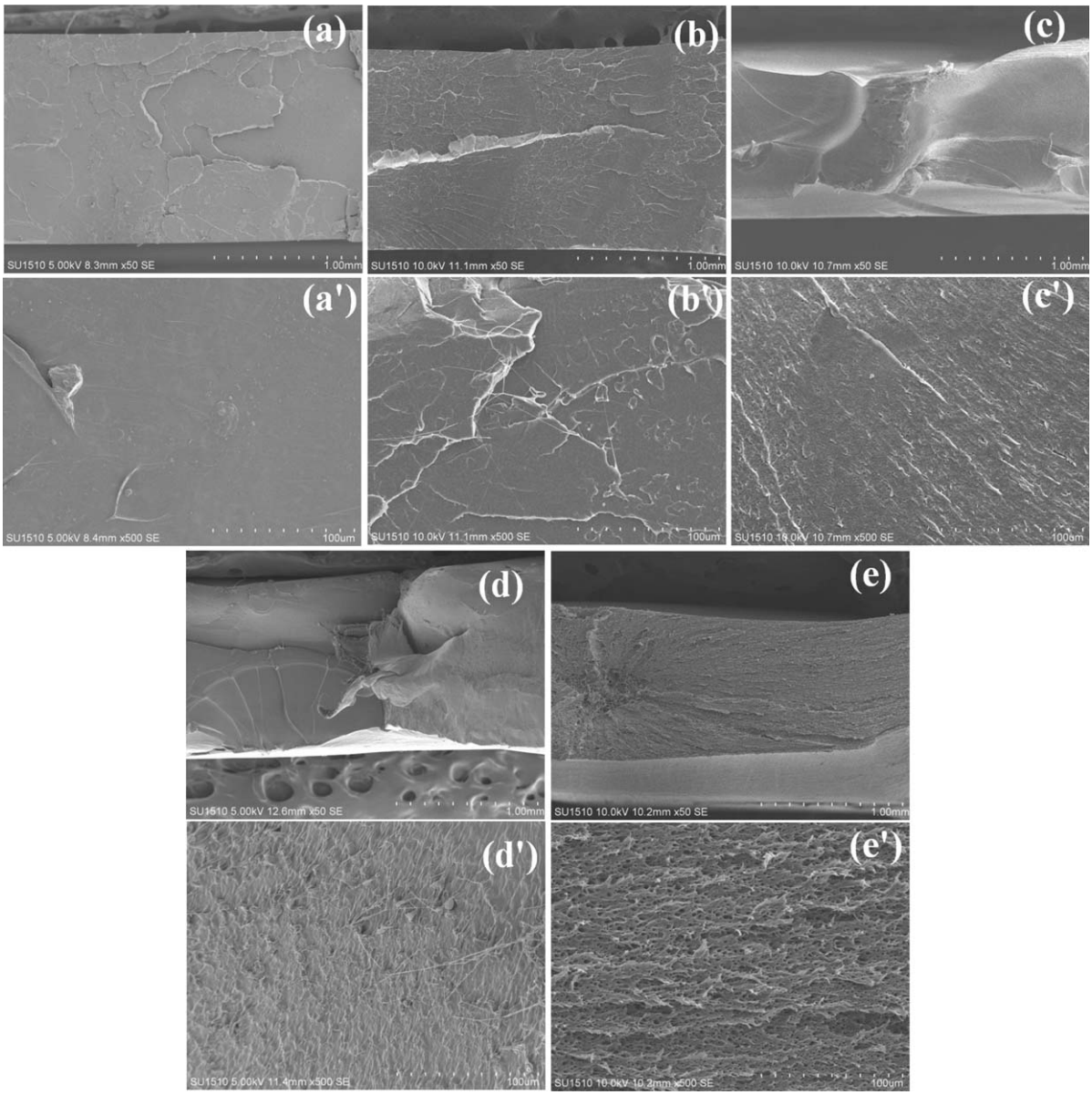

Figure 6. SEM photographs of tensile-fractured cross-section of PLA/PHBV blends and neat PLA. (a, a′) 100/0; (b, b′) 95/5; (c, c′) 90/10; (d, d′) 80/20; and (e, e′) 70/30.

in compressive stress acting on the equatorial plane of PHBV dispersed in PLA matrix under tensile stress. The cold drawing of PHBV particles occurred under the compressive pressure, which resulted in large elongation of PHBV particles and energy absorption. Therefore, the PLA/PHBV blends presented relatively high toughness in comparison with neat PLA.[27]

Figure 7. Optical photographs of sheets of neat PLA and PLA/PHBV blends. (a) PLA/PHBV = 95/5, (b) PLA/PHBV = 90/10, (c) PLA/PHBV = 80/20, and (d) PLA/PHBV = 70/30. [Color figure can be viewed in the online issue, which is available at wileyonlinelibrary.com.]

Optical Transparency

To examine the effect of PHBV on optical transparency of PHBV, sheets were prepared by hot press with sheet thickness of 1 mm. The photographs of sheets of neat PLA and PLA/PHBV blends were shown in Figure 7. Figure 7 showed that neat PLA was completely transparent. The transparency of PLA/PHBV blends was lower than neat PLA. The PLA/PHBV blend with 5 wt % PHBV exhibited high transparency. However, with the increase of PHBV content, the transparency of PLA/PHBV blends decreased gradually. When the content of PHBV was above 10%, PLA/PHBV blends were opaque. The reasons that incorporation of PHBV to PLA caused a transformation from an optical transparent to an opaque system were as followed. On one hand, PLA and PHBV in PLA/PHBV blends were immiscible. The different refractive indices of PLA and PHBV resulted in a decrease of transparency of system.[28,29] On the other hand, it could be known by previous DSC analysis that with the increase of PHBV content, the crystallinity of system increased gradually, which led to a decrease of transparency of system.

CONCLUSIONS

The PLA/PHBV blends with four different ratios (95/5, 90/10, 80/20, and 70/30) were prepared by melt mixing in a microcompounder. The nonisothermal crystallization and melting behavior, miscibility, phase morphology, mechanical property, and optical transparency of neat PLA and PLA/PHBV blends were studied by DSC, FTIR-ATR, SEM, tensile strength test machine, and camera. The results showed that PLA and PHBV in PLA/PHBV blends were immiscible. The weak interaction between PLA and PHBV in PLA/PHBV blends existed. The PHBV was dispersed in PLA matrix uniformly. The interface between PLA and PHBV was obscure. For all the blends with 5–30 wt % PHBV, the size of PHBV domain was less than 2 μm. The addition of PHBV made the crystallization of PLA easier due to PHBV acting as nucleating agent. PLA in PLA/PHBV blends presented various spherulite morphologies different from neat PLA. When the content of PHBV was above 10 wt %, the spherulites with banded structures appeared. In addition, the crystallinity of neat PLA was lower than those of PLA component in PLA/PHBV blends. With the increase of PHBV content in PLA/PHBV blends, the crystallinity of PLA/PHBV blends increased. PHBV could enhance significantly the toughness of PLA. The brittle-to-ductile transition occurred by introducing PHBV to PLA. However, with the increase of PHBV content, the σ_y, E, and ε_y of PLA/PHBV blends decreased gradually. In addition, incorporation of PHBV to PLA caused a transformation from an optical transparent to an opaque system.

ACKNOWLEDGMENTS

This work was supported by National Natural Science Foundation of China (51403084), the Natural Science Foundation of Jiangsu Province (No.BK20130142), the Key Laboratory of Food Colloids and Biotechnology, Ministry of Education, Jiangnan University (JDSJ2013-05), State Key Laboratory of Molecular Engineering of Polymers (Fudan University) (K2015-18), the Open Project Program of Key Laboratory of Yarn Forming and Combination Processing Technology of Zhejiang Province (Jiaxing University) (MTC2014-008), the Industrial Support Program of Suqian (H201313), and the Fundamental Research Funds for the Central Universities of Jiangnan University (JUSRP51417B).

REFERENCES

1. Wu, D.; Yuan, L.; Laredo, E.; Zhang, M.; Zhou, W. *Ind. Eng. Chem. Res.* **2012**, *51*, 2290.
2. Lim, L.-T.; Auras, R.; Rubino, M. *Prog. Polym. Sci.* **2008**, *33*, 820.
3. Solarski, S.; Ferreira, M.; Devaux, E. *Polym. Degrad. Stab.* **2008**, *93*, 707.
4. Liu, Q. S.; Jiang, J. Z.; Zhang, H. X.; Wang, J. C.; Li, X. M.; Li, Y. H.; Deng., B. Y. *Polym. Plast. Technol. Eng.* **2014**, *53*, 1590.
5. Pan, P. J.; Zhu, B.; Inoue, Y. *Macromolecules* **2007**, *40*, 9664.
6. Bitinis, N.; Sanz, A.; Nogales, A.; Verdejo, R.; Lopez-Manchado, M. A.; Ezquerra, T. A. *Soft Matter* **2012**, *8*, 8990.
7. Auras, R.; Lim, L.-T.; Selke, S. E. M.; Tsuji, H. In Poly(lactic acid): Synthesis, Structures, Properties, Processing, and Application; Detyothin, S.; Kathuria, A.; Jaruwattanayon, W.; Selke, S. E. M.; Auras, R., Eds.; Wiley: New Jersey, **2010**; Chapter 20, pp 217–264.
8. Liu, Q. S.; Zhang, H. X.; Zhu, M. F.; Dong, Z.; Wu, C.; Jiang, J. Z.; Li, X. R.; Luo, F.; Gao, Y. X.; Deng, B. Y.; Zhang, Y.; Xing, J.; Wang, H. F.; Li, X. M. *Fiber Polym.* **2013**, *14*, 1688.
9. Liu, Q. S.; Zhang, H. X.; Deng, B. Y.; Zhao, X. Y. *Int. J. Polym. Sci.* **2014**, 374368.
10. Liu, Q. S.; Zhu, M. F.; Deng, B. Y.; Tung, C. H.; Shyr, T.-W. *Eur. Polym. J.* **2013**, *49*, 3937.
11. Liu, Q. S.; Shyr, T.-W.; Tung, C. H.; Liu, Z. H.; Shan, G. F.; Zhu, M. F.; Deng, B. Y. *J. Polym. Res.* **2012**, *19*, 9756.
12. Liu, Q. S.; Shyr, T.-W.; Tung, C. H.; Zhu, M. F.; Deng, B. Y. *Macromol. Res.* **2011**, *19*, 1220.
13. Liu, Q. S.; Deng, B. Y.; Tung, C. H.; Zhu, M. F.; Shyr, T.-W. *J. Polym. Sci. Part B: Polym. Phys.* **2010**, *48*, 2288.
14. Liu, Q. S.; Shyr, T.-W.; Tung, C. H.; Deng, B. Y.; Zhu, M. F. *Fiber Polym.* **2011**, *12*, 848.
15. Liu, Q. S.; Zhu, M. F.; Chen, Y. M. *Polym. Int.* **2010**, *59*, 842.
16. Liu, Q. S.; Zhu, M. F.; Wu, W. H.; Qin, Z. Y. *Polym. Degrad. Stab.* **2009**, *94*, 18.
17. Ma, P. M.; Spoelstra, A. B.; Schmit, P.; Lemstra, P. J. *Eur. Polym. J.* **2013**, *49*, 1523.
18. Zhang, M.; Thomas, N. L. *Adv. Polym. Technol.* **2011**, *30*, 67.
19. Abdelwahab, M. A.; Flynn, A.; Chiou, B.-S.; Imam, S.; Orts, W. *Polym. Degrad. Stab.* **2012**, *97*, 1822.
20. Modi, S.; Koelling, K.; Vodovotz, Y. *J. Appl. Polym. Sci.* **2012**, *124*, 3074.
21. Nanda, M. R.; Misra, M.; Mohanty, A. K. *Macromol. Mater. Eng.* **2011**, *296*, 719.
22. Furukawa, T.; Sato, H.; Murakami, R.; Zhang, J.; Duan, Y.-X.; Noda, I.; Ochiai, S.; Ozaki, Y. *Macromolecules* **2005**, *38*, 6445.

23. Liu, X. B.; Zou, Y. B.; Li, W. T.; Cao, G. P.; Chen, W. *J. Polym. Degrad. Stab.* **2006**, *91*, 3259.
24. Zembouai, I.; Kaci, M.; Bruzaud, S.; Benhamida, A.; Corre, Y.-M.; Grohens, Y. *Polym. Test.* **2013**, *32*, 842.
25. Zhang, J.; Furukawa, T.; Sato, H.; Tsuji, H.; Noda, I.; Ozaki, Y. J. *Phys. Chem.* **2006**, *110*, 24463.
26. Li, X.; Kang, H. L.; Shen, J. X.; Zhang, L. Q.; Nishi, T.; Ito, K.; Zhao, C.; Coates, P. *Polymer* **2014**, *55*, 4313.
27. Kurauchi, T.; Ohta, T. *J. Mater. Sci.* **1984**, *19*, 1699.
28. Choochottiros, C.; Chin, I.-J. *Eur. Polym. J.* **2013**, *49*, 957.
29. Meng, B.; Deng, J. J.; Liu, Q.; Wu, Z. H.; Yang, W. *Eur. Polym. J.* **2012**, *48*, 127.